Downscaling SMOS-Derived Soil Moisture Using MODIS Visible/Infrared Data

María Piles, *Member, IEEE*, Adriano Camps, *Fellow, IEEE*, Mercè Vall-llossera, *Member, IEEE*, Ignasi Corbella, *Senior Member, IEEE*, Rocco Panciera, Christoph Rüdiger, *Member, IEEE*, Yann H. Kerr, *Senior Member, IEEE*, and Jeffrey Walker

***Abstract*—A downscaling approach to improve the spatial resolution of Soil Moisture and Ocean Salinity (SMOS) soil moisture estimates with the use of higher resolution visible/infrared (VIS/IR) satellite data is presented. The algorithm is based on the so-called "universal triangle" concept that relates VIS/IR parameters, such as the Normalized Difference Vegetation Index (NDVI), and Land Surface Temperature (T_s), to the soil moisture status. It combines the accuracy of SMOS observations with the high spatial resolution of VIS/IR satellite data into accurate soil moisture estimates at high spatial resolution. In preparation for the SMOS launch, the algorithm was tested using observations of the UPC Airborne RadIomEter at L-band (ARIEL) over the Soil Moisture Measurement Network of the University of Salamanca (REMEDHUS) in Zamora (Spain), and LANDSAT imagery. Results showed fairly good agreement with ground-based soil moisture measurements and illustrated the strength of the link between VIS/IR satellite data and soil moisture status. Following the SMOS launch, a downscaling strategy for the estimation of soil moisture at high resolution from SMOS using MODIS VIS/IR data has been developed. The method has been applied to some of the first SMOS images acquired during the commissioning phase and is validated against *in situ* soil moisture data from the OZnet soil moisture monitoring network, in South-Eastern Australia. Results show that the soil moisture variability is effectively captured at 10 and 1 km spatial scales without a significant degradation of the root mean square error.**

***Index Terms*—Downscaling algorithm, MODIS, passive microwave remote sensing, SMOS, soil moisture, spatial resolution.**

Manuscript received July 1, 2010; revised November 30, 2010 and February 7, 2011; accepted February 13, 2011. Date of publication April 29, 2011; date of current version August 26, 2011. This work was supported by the Spanish Ministry of Science and Education under the FPU Grant AP2005-4912 and projects ESP2007-65667-C04-02, AYA2009-06844-E and AYA2010-22062-C05-05/ESP. Additional support came from the University of Melbourne through an early career research Grant to R. Panciera and C. Rüdiger, and from the Australian Research Council Discovery Projects DP0879212, DP0557543, and DP0343778.

M. Piles was with the Remote Sensing Laboratory, Department of Signal Theory and Communications, Universitat Politècnica de Catalunya, 08034, Barcelona, Spain, and IEEC/CRAE-UPC, 08034 Barcelona, Spain, and also with the SMOS Barcelona Expert Center, 08003 Barcelona, Spain. She is now at the Department of Civil and Environmental Engineering, University of Melbourne, Melbourne, Vic. 3010, Australia (e-mail: maria.piles@tsc.upc.edu).

A. Camps, M. Vall-llossera and I. Corbella are with the Remote Sensing Laboratory, Department of Signal Theory and Communications, Universitat Politècnica de Catalunya, 08034, Barcelona, Spain, and IEEC/CRAE-UPC, 08034 Barcelona, Spain, and also with the SMOS Barcelona Expert Center, 08003 Barcelona, Spain (e-mail: camps@tsc.upc.edu; merce@tsc.upc.edu; corbella@tsc.upc.edu).

R. Panciera is with Department of Civil and Environmental Engineering, University of Melbourne, Melbourne, Vic. 3010, Australia (e-mail: panr@unimelb.edu.au).

C. Rüdiger and J. Walker are with Department of Civil Engineering, Monash University, Clayton, Vic. 3800, Australia (e-mail: chris.rudiger@monash.edu; jeff.walker@monash.edu).

Y. H. Kerr is with Centre d'Etudes Spatiales de la Biosphère, CNES, 31401 Toulouse, France (e-mail: yann.kerr@cesbio.cnes.fr).

Color versions of one or more of the figures in this paper are available online at http://ieeexplore.ieee.org.

Digital Object Identifier 10.1109/TGRS.2011.2120615

I. Introduction

THEORETICAL, ground-based, and airborne experimental studies have proven that L-band passive remote sensing is optimal for soil moisture sensing due to its all-weather capabilities and the high sensitivity of the land emission to soil moisture under most vegetation covers [1]–[3]. The ESA Soil Moisture and Ocean Salinity (SMOS) mission, in orbit since November the 2nd 2009, and the NASA Soil Moisture Active Passive (SMAP) mission, to be launched in 2014, are the first ever L-band satellites dedicated to the global measurement of the Earth's near-surface soil moisture. The SMOS payload is a novel L-band 2-D interferometric radiometer that provides accurate brightness temperature measurements of the Earth at different polarizations and incidence angles, with a spatial resolution of $\sim$50 km [4]. The spatial resolution of SMOS observations is adequate for many global applications, but restricts the use of the data in regional studies over land, where a resolution of 1–10 km is needed [5], [6]. The SMAP payload, in turn, consists on a L-band radiometer and a high-resolution radar to improve the spatial resolution of the soil moisture retrievals up to 10 km [7]–[9].

In this context, the combination of SMOS data with higher resolution data coming from other sensors offers a potential solution to decompose or disaggregate global soil moisture estimates to the higher resolution required. The possibility of using visible/infrared (VIS/IR) sensors for soil moisture sensing has been widely studied in the past, since VIS/IR sensors onboard satellites provide good spatial resolution, and controlled experiments have shown their potential to sense soil moisture [10]–[13]. However, they are equally sensitive to soil types, and it is difficult to decouple the two signatures. In addition, soil moisture estimates from VIS/IR sensors usually require surface micro-meteorological and atmospheric information that is not routinely available [14], [15]. Hence, VIS/IR sensors are commonly used to provide an indirect measurement of soil moisture, but not to retrieve it.

To achieve accuracy and high spatial resolution, it seems natural to try to combine the strength of the microwave and

0196-2892/$26.00 © 2011 IEEE

VIS/IR approaches for soil moisture estimation. Recently, a number of studies have documented the emergence of a triangular or trapezoidal shape when remotely sensed surface radiant temperature (T_s) over heterogeneous areas are plotted versus vegetation index (VI) measurements; an analysis of this "universal triangle" has led to different methods relating the T_s/VI space to land surface energy fluxes and surface soil moisture. A comprehensive review of these methods can be found in [16] and [17]. Particularly, an algorithm for the operational retrieval of high-resolution surface soil moisture from future Visible Infrared Imager Radiometer Suite (VIIRS) and Microwave Imager Sounder (MIS) data, under the National Polar-Orbiting Operational Environmental Satellite System (NPOESS), is underway [18]. It has a definite theoretical basis that links soil moisture to the T_s/VI space [19], and was demonstrated using 1 km AVHRR and 25 km SSM/I in [20]. A variant of this method for SMOS using 1 km MODerate resolution Imaging Spectroradiometer (MODIS) data, soil dependent parameters, and wind speed data is presented in [21]. As an alternative to these empirically-based approaches, a physically-based algorithm that includes a complex surface process model and high resolution multispectral data and surface variables involved in a land-surface-atmosphere model is presented in [22]. This method is simplified using an energy balance model in [23]. However, the applicability of these algorithms to the upcoming space-borne observations is limited to the availability of the soil and vegetation parameters they need at global scale.

An algorithm to synergistically combine SMOS soil moisture estimates and MODIS VIS/IR data into high resolution soil moisture is presented in this paper. As part of the downscaling activities conducted at the REMEDHUS Calibration/Validation (Cal/Val) site, the possibility of improving the spatial resolution of passive L-band airborne observations using VIS/IR data from LANDSAT was explored. Results showed reasonable agreement with ground-based soil moisture observations, and illustrated the strength of the link between VIS/IR satellite data and soil moisture status [24]. Following these first experiments, a downscaling strategy to improve the spatial resolution of SMOS soil moisture estimates using MODIS-derived NDVI and T_s data has been developed. MODIS has been selected among other operational VIS/IR satellites for its suitable characteristics, mainly, its temporal resolution (1–2 days), data availability (near real time), spatial resolution (1 km), and overpass time (10:30 A.M. for MODIS/Terra, 1:30 P.M. for MODIS/Aqua). Alternatives present severe incompatibilities to be used in combination with SMOS measurements such as the 16-days repeat cycle of ASTER and LANDSAT. Still, it is important to outline the limitations of using MODIS VIS/IR for downscaling SMOS soil moisture data. First, the sensing depth of SMOS L-band for bare soil is $\sim$5 cm, whereas for the MODIS thermal infrared band is $\sim$1 mm. Note that the thermal regime of 0–5 cm and of 0–1 mm (skin) are likely to be quite different, since the skin temperature is subject to rapid fluctuations and more correlated to ambient temperature as compared to 0–5 cm integrated soil temperature. The usage of skin temperature in the algorithm could then lead to misrepresentation of spatial and temporal variability of underlying soil temperature for 0–5 cm depth. Also, note that L-band can penetrate moderately vegetated regions (up to 5 kg/m^2) but thermal infrared cannot sense through a vegetation layer. Second, the thermal regime of top 0–5 cm soil profile is almost the same at 6:00 A.M. (SMOS overpass), but may digress at 10.30 (MODIS/Terra overpass), and soil moisture status may change within these two acquisition times depending upon soil type, terrain, vegetation and meteorological conditions. Nonetheless, as it will be presented later in this paper, the use of MODIS data in this study provides valuable information for improving the spatial resolution of SMOS soil moisture estimates.

The downscaling approach builds on the VIIRS concept in [18]: it consists of aggregating high resolution VIS/IR land surface parameters to the scale of the microwave observations for the purpose of building a linking model that is afterwards applied at fine scale to disaggregate the passive soil moisture observations into high-resolution soil moisture. This approach has been specifically adapted to SMOS, and uses a novel linking model to strengthen the relationship between land surface parameters and soil moisture, which is needed to capture soil moisture variability at fine scale. Details of the SMOS, MODIS, and ground-based data used in this study are presented in Section II. The downscaling method is fully described in Section III. Results of its application to some of the first SMOS images acquired over the Murrumbidgee catchment, in South-Eastern Australia, during the commissioning phase (January 17 to February 22, 2010) are provided in Section IV. The spatial variability of SMOS-derived soil moisture observations is effectively captured at the spatial resolutions of 40, 10, and 1 km, and soil moisture estimations are compared to *in situ* soil moisture data to evaluate the accuracy of the observations at the different spatial scales. Further studies with airborne data at an intermediate resolution are ongoing to fully assess the radiometric accuracy of the observations and to establish a downscaling limit, which could be given either by the resolution of the optical sensor (which in the case of MODIS is 1 km), or by the presence of noise affecting the accuracy of the soil moisture estimates. In Section V, the main findings and contributions of this work are summarized, and the operational applicability of this downscaling strategy to SMOS is discussed.

II. Data Description

A. Ground-Based Soil Moisture

Ground-based measurements of 0–5 cm volumetric soil moisture from the OzNet permanent soil moisture monitoring network (www.oznet.unimelb.edu.au), in the Murrumbidgee catchment (-33 to -37 S, 143 to 150 E), South-Eastern Australia [Fig. 1(a)], are used to evaluate the algorithm performance. The chosen study period is from January 17 to February 22, 2010, so that airborne and intensive soil moisture measurements from the Australian Airborne Cal/Val Experiments for SMOS (AACES) are available for future studies [25]. The comparison of SMOS-derived soil moisture estimates to ground-truth data is focused on a subset of those stations, located within the Coleambally Irrigation Area, South of Yanco (referred hereafter as the Yanco region). It is a

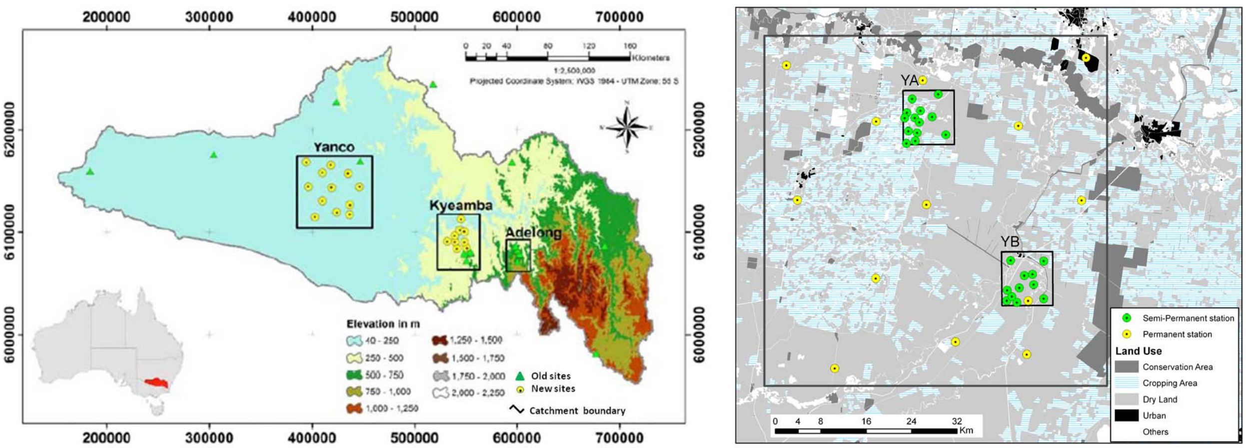

(a) (b)

Fig. 1. (a) Murrumbidgee catchment showing elevation and permanent soil moisture monitoring network. (b) Layout of the permanent and semi-permanent soil moisture stations within the Yanco intensive monitoring region.

semi-arid agricultural area of approximately 60 km by 60 km (∼ a SMOS pixel), characterized by flat topography; its land use is mainly grazing dry lands with occasional winter crops (wheat, barley, oats, and canola) [26]. The Yanco intensive study area hosts a network of 13 permanent soil moisture stations deployed all over the region and 24 additional semi-permanent stations focused in two 9 × 9 km areas [YA and YB in Fig. 1(b)]. Semi-permanent stations are a recent upgrade to the OzNet monitoring network for the specific purpose of SMAP algorithm development and Cal/Val studies (SMAPEx project http://smap.jpl.nasa.gov/science/Validation/SMAPEx/).

B. SMOS Data

SMOS soil moisture images derived from preliminary brightness temperatures obtained during the commissioning phase and a pre-operational prototype of the L2 processor are used in the present study. These soil moisture maps do include biases and errors, which are due to the lack of maturity of the processor at the time of the campaign. However, the values should be seen as indicative, not as absolute, and the results of the study are not compromised by these errors. Soil moisture maps are from January 17, 19, 25, 27, and 29, and February 3, 6, 9, 14, 16, 17, 19, and 21, 2010, which are the days with overlapping SMOS and cloud-free MODIS data in the Murrumbidgee catchment (see Table I). Only ascending SMOS data has been used in this study, since the thermal equilibrium and near uniform conditions in surface soil layers and overlying vegetation needed for soil moisture retrieval are more likely to be true at 6 A.M. than at 6 P.M.; this can be critical in the early-stage of the SMOS mission in which we are now. SMOS L1c browse products, which contain observations acquired at a constant incidence angle of 42.5° [27], are also used in this study as auxiliary information. For an initial validation of the algorithm, only horizontally polarized L1c brightness temperatures are considered, since horizontal polarization is more sensitive to soil moisture variations than vertical polarization [28].

Note that the resolution of SMOS observations varies from 30 km at nadir to ∼90 km at the upper borders of the FOV. In this paper, SMOS observations are combined on a regular grid of 40 × 40 km and are downscaled to grids of 10 and 1 km spatial resolution.

TABLE I
LIST OF THE 16-DAY MODIS NDVI COMPOSITES AND THE OVERLAPPING SMOS SOIL MOISTURE MAPS AND CLOUD FREE MODIS T_s DATA USED IN THIS STUDY. DATES ARE IN UTC

Day of year 2010	SMOS (6 am)	MODIS/Terra T_s(10.30 am)	MODIS/Aqua T_s(1.30 pm)	MODIS NDVI
Jan 17	✓	–	✓	✓
Jan 19	✓	✓	✓	–
Jan 25	✓	✓	✓	–
Jan 27	✓	✓	✓	–
Jan 29	✓	✓	✓	–
Feb 2	–	–	–	✓
Feb 3	✓	✓	–	–
Feb 6	✓	✓	–	–
Feb 9	✓	–	✓	–
Feb 14	✓	–	✓	–
Feb 16	✓	–	✓	–
Feb 17	✓	✓	✓	–
Feb 18	–	–	–	–
Feb 19	✓	✓	✓	✓
Feb 21	✓	✓	✓	–

C. MODIS Data

The MODIS instrument operates on both the Terra (10:30 A.M./10:30 P.M.) and Aqua (1:30 A.M./1:30 P.M.) spacecrafts. The MODIS data used in this work are the version 5 MODIS/Terra and MODIS/Aqua 1 km resolution daily daytime T_s, and MODIS/Terra 1 km resolution 16-day NDVI product (data sets MOD11A1, MYD11A1, and MOD13A2, respectively). The NDVI composite is cloud free, whereas the T_s is not. The option of using the 8-day T_s composite was discarded, since it is not as representative as the actual T_s and it is not cloud free in all cases. MODIS products are freely distributed by the U.S. Land Processes Distributed Active Archive Center (lpdaac.usgs.gov). Table I lists the days with overlapping SMOS soil moisture successful retrievals and cloud free MODIS T_s data during the AACES field experiment.

III. METHOD

The downscaling method for the estimation of soil moisture at high resolution from SMOS soil moisture data using

MODIS-derived T_s and NDVI data consists of two main steps, which are described in the following sections.

A. Step 1: Linking Model

A linking model based on the triangle concept has been developed to relate SMOS soil moisture maps to MODIS-derived NDVI and T_s (aggregated to 40 km).

Theoretical and experimental studies have demonstrated that there can be a unique relationship between soil moisture (s_m), NDVI, and T_s for a given region under specific climatic conditions and land surface types. This relationship can be expressed through a regression formula such as [19]

$$s_m = \sum_{i=0}^{n} \sum_{j=0}^{n} a_{ij} \mathrm{NDVI}^i \, T_s^j \tag{1}$$

where n should be chosen so as to give a reasonable representation of the data.

In [24], the following approximation of (1) was effectively used to define the linking model between the LANDSAT T_s/NDVI space and airborne soil moisture estimates

$$s_m = a_{00} + a_{01}T_N + a_{10}F_r + a_{11}T_N F_r + a_{02}T_N^2 + a_{20}F_r^2 \tag{2}$$

where T_N stands for normalized LANDSAT surface radiant temperature and F_r is the fractional vegetation cover [29], defined as

$$T_N = \frac{T_s - T_{min}}{T_{max} - T_{min}} \tag{3}$$

$$F_r = \frac{\mathrm{NDVI} - \mathrm{NDVI}_{min}}{\mathrm{NDVI}_{max} - \mathrm{NDVI}_{min}} \tag{4}$$

with T_{max} and T_{min} being the maximum and minimum T_s values for a particular day and region under study, and, similarly, NDVI_{max} and NDVI_{min} being the maximum and minimum NDVI values for a particular day and scene. Normalization is needed to reduce the dependence of T_s/NDVI on ambient conditions, and to allow further comparison of different experiments.

In the context of SMOS, SMOS brightness temperatures T_B have been added to the right side of (1) to strengthen the relationship between land surface parameters and soil moisture. Thus, (1) is modified to

$$s_m = \sum_{i=0}^{n} \sum_{j=0}^{n} \sum_{k=0}^{n} a_{ijk} \mathrm{NDVI}^i T_s^j T_B^k. \tag{5}$$

SMOS T_B include information on all parameters that dominate the Earth's emission at L-band, in addition to soil moisture, e.g., soil roughness, soil texture, soil temperature, vegetation opacity and vegetation scattering albedo. As it will be shown later in the paper, the use of brightness temperatures in the linking model is needed to capture soil moisture variability at high resolution, and to reproduce changes in soil moisture due to rain events being detected by SMOS at 6 A.M. but not by MODIS/TERRA at 10:30 A.M. or MODIS/AQUA at 1:30 P.M.

Using (3) and (4), the following approximation of (5) has been defined as linking model between SMOS observations and MODIS-derived NDVI and T_s data

$$\begin{aligned} s_m = {} & a_{000} + a_{001}T_{BN} + a_{010}T_N + a_{100}F_r \\ & + a_{002}T_{BN}^2 + a_{020}T_N^2 + a_{200}F_r^2 + a_{011}T_N T_{BN} \\ & + a_{101}F_r T_{BN} + a_{110}F_r T_N \end{aligned} \tag{6}$$

where T_{BN} are the normalized SMOS brightness temperatures

$$T_{BN} = \frac{T_B - T_{Bmin}}{T_{Bmax} - T_{Bmin}} \tag{7}$$

with T_{Bmax} and T_{Bmin} being the maximum and the minimum T_B values for a particular day and region under study.

Three main semi-empirical relationships can be found in literature to derive vegetation fraction from NDVI: [29]–[31]. No significant differences have been found on the algorithm performance when using these three alternatives, and [29] has been adopted for simplicity.

The linking model in (6) is used to set up a system of linear equations for all the pixels in the image. This system is solved to obtain the regression coefficients a_{ijk}—which are specific of the day and scene being analyzed.

B. Step 2: High Resolution Soil Moisture

SMOS-derived soil moisture maps at 10 km are obtained by applying (6) with the regression coefficients a_{ijk} (from step 1), T_N and F_r aggregated to 10 km, and SMOS T_{BN} resampled to a 10 × 10 km grid. Similarly, soil moisture maps at 1 km are obtained by applying (6) with the regression coefficients a_{ijk}, T_N and F_r at 1 km, and SMOS T_{BN} resampled to a 1 × 1 km grid.

It is important to note that T_N, F_r and T_{BN} at low (40 km) and high (1–10 km) spatial resolution should be computed so as to have the same mean value within every 40 km pixel. This ensures that the downscaled soil moisture has the same mean value that the 40 km SMOS L2 soil moisture product.

IV. RESULTS

The downscaling algorithm described in Section III has been applied to all the SMOS soil moisture and cloud-free MODIS AQUA/TERRA T_s overlapping images during AACES field experiment (20 images in total, see SMOS—MODIS T_s combinations in Table I). In this section, soil moisture maps at 10 and 1 km spatial resolution, resulting from the application of the downscaling algorithm proposed, are analyzed. Results of using (2) instead of (6) have been included so as to compare the effect of adding or not SMOS T_B to the linking model. An insight of the coupling between MODIS VIS/IR parameters and SMOS-derived soil moisture is given. Finally, soil moisture estimates at 40, 10, and 1 km are compared to *in situ* soil moisture data from the Yanco region [see Fig. 1(b)], to validate the accuracy of the observations at the different spatial scales.

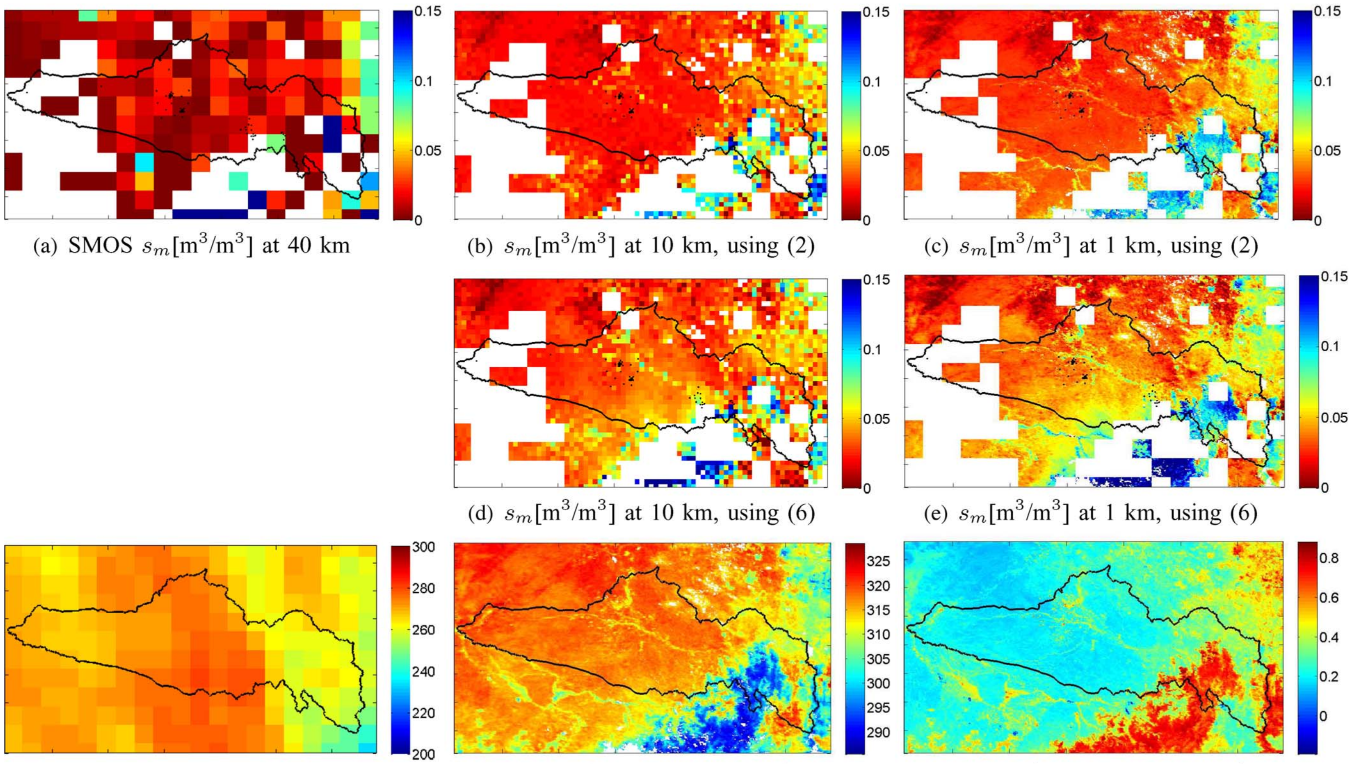

(a) SMOS s_m[m^3/m^3] at 40 km (b) s_m[m^3/m^3] at 10 km, using (2) (c) s_m[m^3/m^3] at 1 km, using (2)

(d) s_m[m^3/m^3] at 10 km, using (6) (e) s_m[m^3/m^3] at 1 km, using (6)

(f) SMOS T_B[K] at 40 km (g) MODIS/AQUA T_s[K] at 1 km (h) MODIS/TERRA NDVI at 1 km

Fig. 2. Results of the application of the algorithm to a SMOS image over the Murrumbidgee catchment, from January 19, 2010 (6 A.M.). (a) SMOS soil moisture [m^3/m^3] on a 40 × 40 grid. SMOS-derived soil moisture maps [m^3/m^3] at (b) 10 km, and (c) 1 km, using the linking model in (2). SMOS-derived soil moisture maps [m^3/m^3] at (d) 10 km, and (e) 1 km, using the linking model in (6). Dots indicate the location of the soil moisture permanent stations within the Murrumbidgee catchment. (f) SMOS T_{Bh} image [K] on a 40 × 40 km grid. (g) 1 km MODIS/AQUA T_s [K]. (h) 1 km MODIS/TERRA NDVI. Empty areas in the images correspond to unsuccessful SMOS soil moisture retrievals, or clouds masking MODIS T_s measurements.

Note that the date on the SMOS and MODIS images used in this Section are expressed in UTC, whereas the satellite overpass is expressed in local time.

A. Soil Moisture Maps

Sample results of the application of the downscaling algorithm to a SMOS soil moisture image over the Murrumbidgee catchment, from January 19, 2010, are shown in Fig. 2. It can be observed that the downscaling method using (2) or (6) nicely captures the spatial patterns in soil moisture at both 10 and 1 km spatial resolutions. Note for instance how spatial details such as the Murrumbidgee river basin can clearly be distinguished, specially when adding the SMOS T_B to the linking model [Fig. 2(d) and (e)].

Fig. 3 shows the results of applying the downscaling algorithm to a SMOS soil moisture image over the Murrumbidgee catchment, from February 21, 2010, when a significant rainfall event occurred over the western part of the catchment, between 4 and 9 A.M. local time (www.oznet.unimelb.edu.au). The significant gradient in soil moisture that can be seen in the SMOS soil moisture map [Fig. 3(a)] and in SMOS T_B [Fig. 3(f)] evidences that this rainfall was effectively captured by SMOS. This gradient is reproduced at the higher spatial resolutions of 10 and 1 km when using the linking model in (6) [see Fig. 3(d) and (e)], but it is not when using the linking model in (2) [see Fig. 3(b) and (c)]. This may be due to the different acquisition times of SMOS and MODIS, i.e., the rainfall being captured by SMOS at 6 A.M., but not being captured either by MODIS/TERRA at 10:30 A.M. Hence, these results clearly show that adding SMOS T_B to the linking model strengthens the coupling between MODIS VIS/IR parameters and SMOS data, which could be critical to effectively reproduce soil moisture dynamics at higher spatial resolutions.

B. $T_s/NDVI$ Space

T_s and NDVI are proven indicators of the vegetative and thermal state of the land surface. Fig. 4 illustrates the polygonal correlation between MODIS T_s and NDVI observations on Fig. 2 [Fig. 4(a)], and Fig. 3 [Fig. 4(b)]. The polygon's edges can be interpreted as the minimum/maximum reached by vegetation cover (NDVI) and soil moisture: bare soil, maximum biomass, completely dry, and fully wet soil surface. The warm edge of the triangle is generally interpreted as representing limiting conditions of soil moisture or evapotranspiration, in contrast to the cold edge, which represents maximum evapotranspiration and thereby unlimited water access. Therefore, the warmest and coldest pixels are usually referred to as the dry and wet edges of the triangle, respectively. Note that this approach is valid under the assumption that changes in evapotranspiration are primarily caused by variations in water availability, and not by differences in atmospheric conditions.

In Fig. 4(a), there is a higher number of pixels along the maximum biomass edge, if compared to the image on Fig. 4(b).

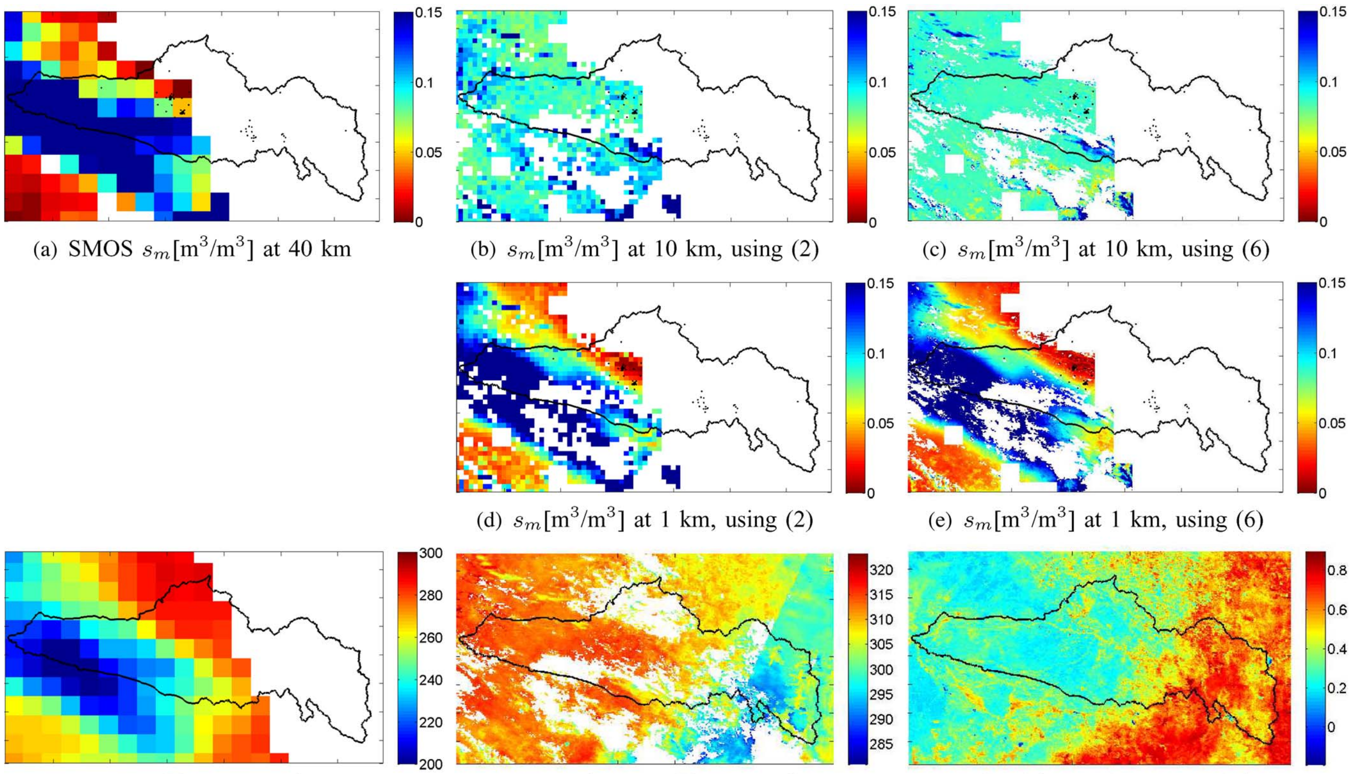

(a) SMOS s_m[m^3/m^3] at 40 km (b) s_m[m^3/m^3] at 10 km, using (2) (c) s_m[m^3/m^3] at 10 km, using (6)

(d) s_m[m^3/m^3] at 1 km, using (2) (e) s_m[m^3/m^3] at 1 km, using (6)

(f) SMOS T_B[K] at 40 km (g) MODIS/TERRA T_s[K] at 1 km (h) MODIS/TERRA NDVI at 1 km

Fig. 3. As for Fig. 2, but using an SMOS image over the Murrumbidgee catchment, from February 21, 2010 (6 A.M.), and MODIS/TERRA T_s. (a) SMOS $s_m[\text{m}^3/\text{m}^3]$ at 40 km; (b) $s_m[\text{m}^3/\text{m}^3]$ at 10 km, using (2); (c) $s_m[\text{m}^3/\text{m}^3]$ at 10 km, using (6); (d) $s_m[\text{m}^3/\text{m}^3]$ at 1 km, using (2); (e) $s_m[\text{m}^3/\text{m}^3]$ at 1 km, using (6); (f) SMOS T_B[K] at 40 km; (g) MODIS/TERRA T_s[K] at 1 km; (h) MODIS/TERRA NDVI at 1 km.

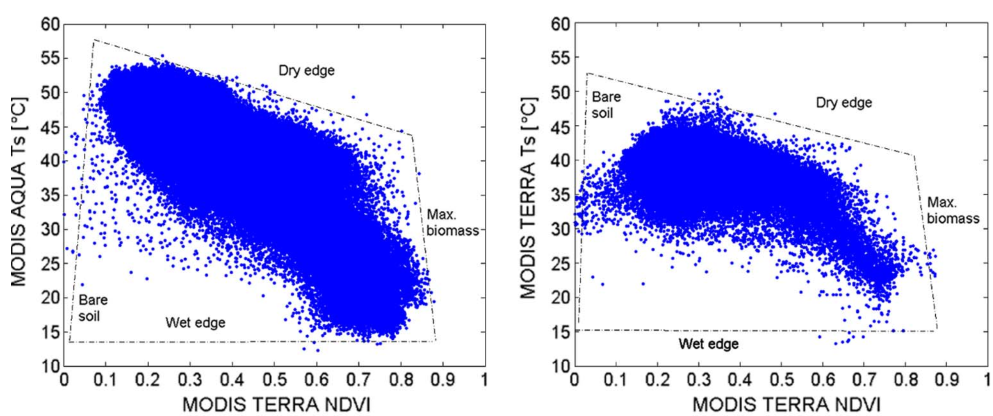

(a) (b)

Fig. 4. Scatter plots of MODIS surface radiant temperature versus MODIS NDVI, from (a) Fig. 2 and (b) Fig. 3.

This is because the Eastern part of the catchment—which contains the highest vegetated areas—is not covered by SMOS on February 21, 2010, and therefore is not used to build the linking model in Fig. 4(b). Also, note that the maximum biomass edge is shorter than the bare soil edge in the two scatter plots, which evidences the low sensitivity of vegetation temperature to changes in soil moisture and the higher sensitivity of bare soil to changes in soil moisture content; the range of T_s decreases as the vegetation cover increases. Another salient aspect of the polygons is that the dry edges slope toward lower temperatures with increasing NDVI, which can be explained by the fact that sunlit vegetation is generally cooler than sunlit bare soil.

The theory behind the triangle concept states that a large number of points (NDVI, T_s pairs) reflecting a full range of soil surface wetness and fractional vegetation cover is needed to identify a triangular shape in the pixel distribution. Hence, the perfect triangle can only be achieved by collecting a timely record of data over the region under study, or by selecting a particular scene with a wide range of T_s and NDVI. This is the most severe limitation of the triangle concept, since some subjectivity may be needed in identifying the dry edge (or warm edge) and the bare soil and maximum biomass extremes when there is not a triangle populated with points [16]. In this paper, however, the edges of the polygon have been detected automatically from MODIS data, and results show that the fact of not

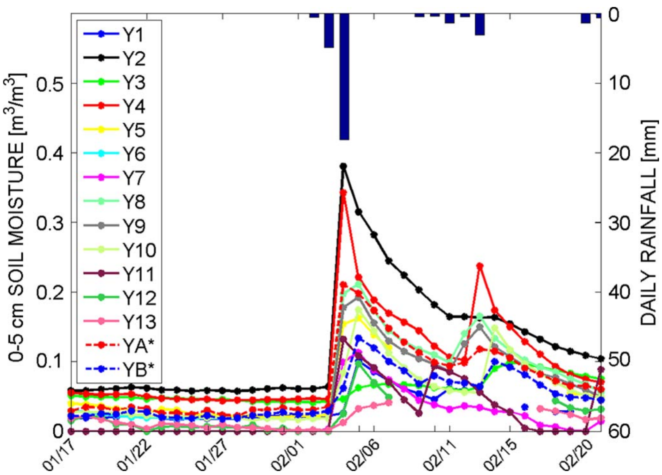

Fig. 5. Temporal evolution of 0–5 cm continuous soil moisture measurements (6 A.M.) and mean daily rainfall observed at 13 Yanco monitoring stations. YA* is the mean of the 13 semi-permanent soil moisture stations within region YA, and YB* is the mean of the 11 semi-permanent soil moisture stations within region YB.

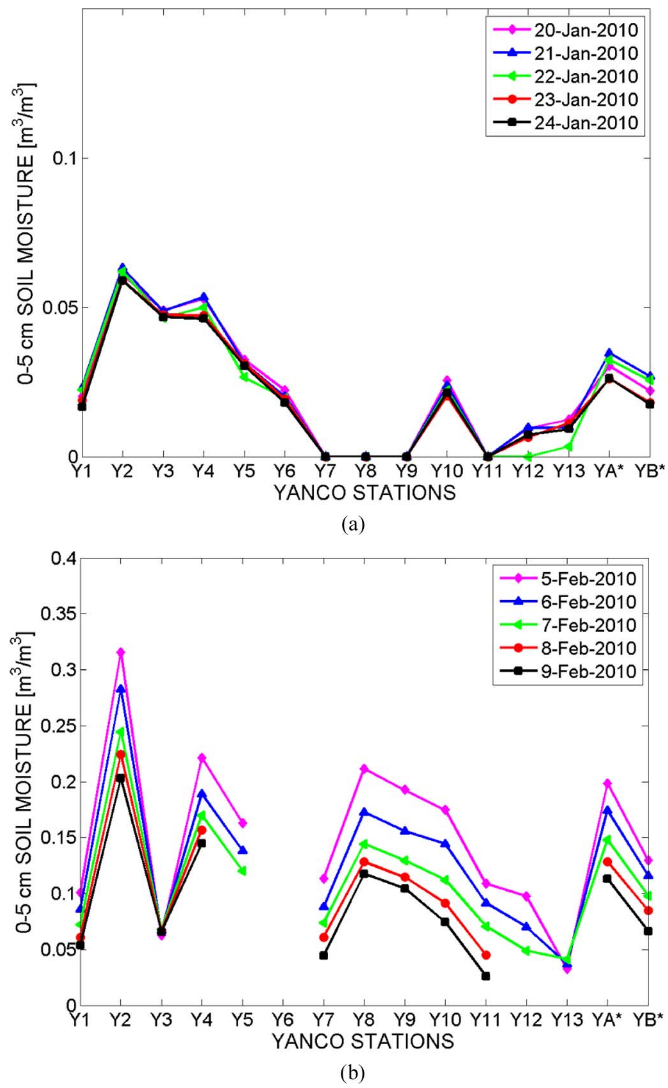

Fig. 6. Spatial variability of 0–5 cm soil moisture measurements (6 A.M.) of the 13 Yanco stations on days (a) January 20–24, 2010, and on (b) February 5–9, 2010.

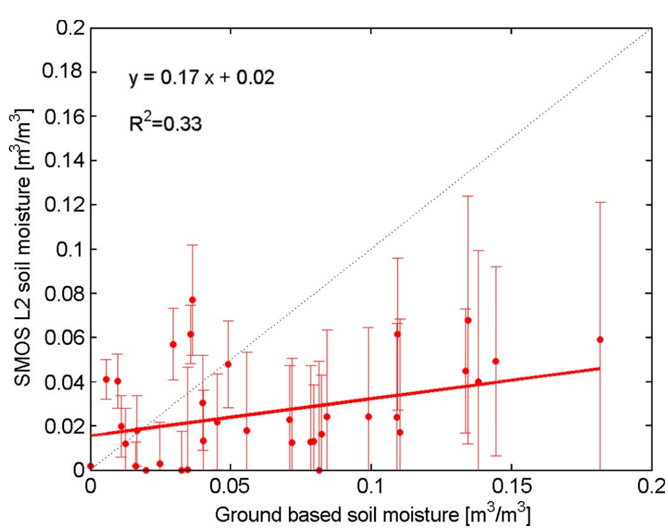

Fig. 7. SMOS soil moisture data over the Yanco region versus 40 km aggregated *in situ* measurements, for the 20 SMOS–MODIS T_s combinations in Table I. Vertical errorbars represent the standard deviation of ground measurements within each 40 km pixel.

having a clearly defined triangular T_s–NDVI pixel distribution in the region under study is not affecting the performance of the algorithm. Nevertheless, this should be certainly taken into account when selecting the extent of the scene under study.

C. Comparison With In Situ Measurements

During the AACES field experiment, soil moisture conditions ranged from extremely hot dry (0 m^3/m^3) to cool wet (0.4 m^3/m^3). Results of applying the downscaling algorithm to the 20 SMOS soil moisture—MODIS T_s combinations in Table I are compared to *in situ* soil moisture measurements within the Yanco region [Fig. 1(b)], so that the performance of the algorithm is assessed in a wide range of moisture conditions.

It is important to remark that validating soil moisture estimation results is not straight-forward, since there are some unresolved issues concerning the comparison of spatially distributed *in situ* measurements with soil moisture maps. The difficulty lies not only in the estimation process, but also in the representativeness of the *in situ* soil moisture measurements. Note that the penetration depth of the microwave signal depends on the soil moisture content itself. Therefore, the thickness of the soil layer contributing to the emitted radiation can significantly vary with moisture conditions. This fact could affect the representativeness of the soil moisture samples taken at a specific depth regardless of the surface conditions. In addition to this, the spatial distribution of soil moisture depends on soil parameters that are not distributed homogeneously in the area (e.g., soil texture, vegetation, and topography). And also, it should be taken into account that soil moisture could change very rapidly in the top layer. In view of these uncertainties, a study of the temporal and spatial variability of the 37 Yanco soil moisture stations has been performed to analyze the consistency of the *in situ* data and, to some extent, of the validation approach.

The temporal variability of soil moisture measurements and the mean daily rainfall at Yanco stations from January 17 to February 21, 2010, is shown in Fig. 5. It can be seen how the

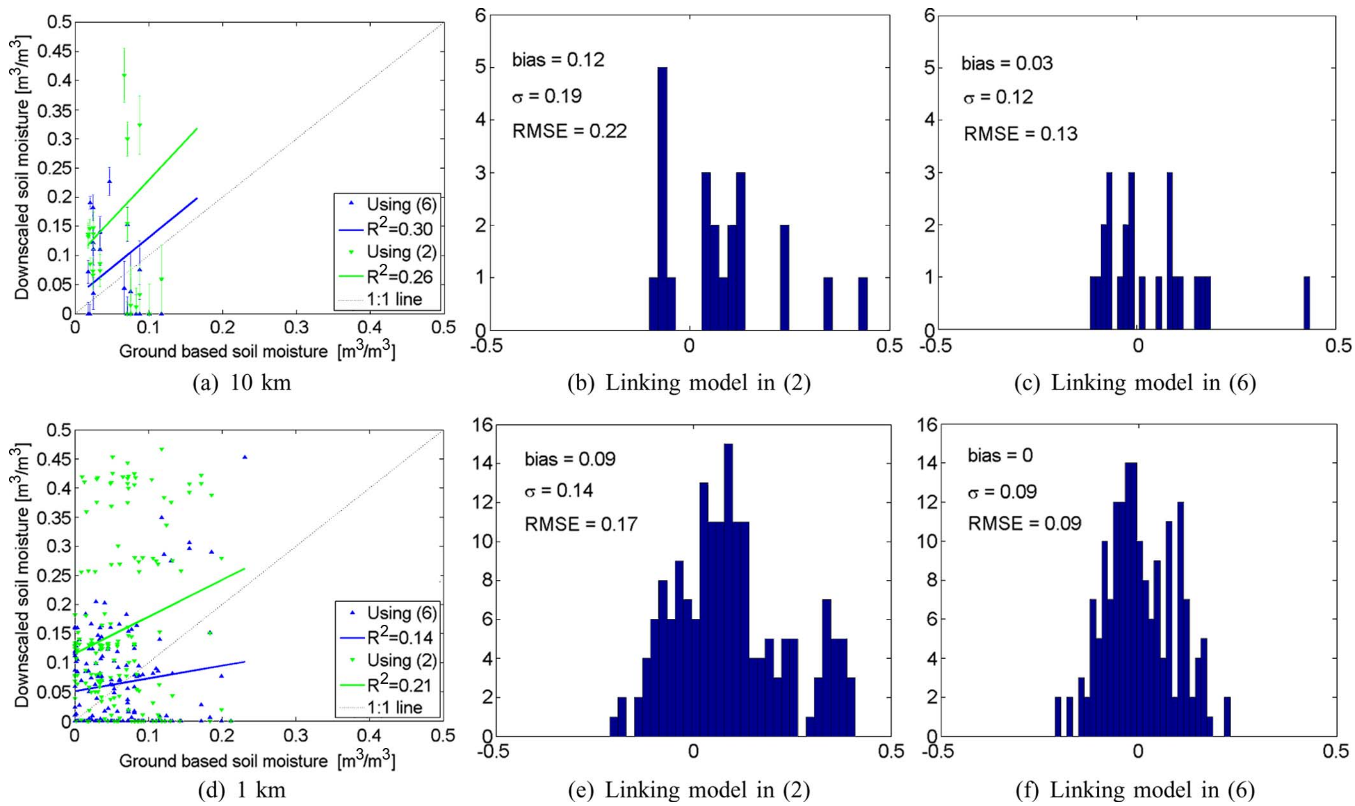

Fig. 8. (a) Downscaled SMOS re-scaled soil moisture data at 10 km versus 10 km aggregated *in situ* measurements, for the 20 SMOS–MODIS T_s combinations in Table I. Vertical errorbars represent the standard deviation of ground measurements within each 10 km pixel. Histograms of the difference between 10 km downscaled soil moisture and *in situ* measurements (b) using the linking model in (2), and (c) using the linking model in (6). (d) Downscaled SMOS L2 calibrated soil moisture data at 1 km versus 1 km aggregated *in situ* measurements, for the 20 SMOS–MODIS T_s combinations in Table I. Vertical errorbars represent the standard deviation of ground measurements within each 1 km pixel. Histograms of the difference between 1 km downscaled soil moisture and *in situ* measurements (e) using the linking model in (2), and (f) using the linking model in (6).

soil moisture network nicely captures the three rainfall events occurred during these days. Fig. 6 shows the measured soil moisture variability at Yanco stations under dry [January 20–24 (a)] and wet [February 5–9 (b)] soil conditions. It can be observed that there is a definite pattern in the spatial variability of soil moisture that repeats itself on all Yanco stations on these two different periods studied. This variability could be the result of changing soil properties of the area. Note that this pattern is common for the case of extremely dry and moderately dry conditions of Fig. 6(a) and (b), respectively, on all the stations except for numbers 8, 9, and 12. Still, the spatial variability appears to be consistent.

SMOS soil moisture retrievals over the Yanco region are plotted against 40 km aggregated *in situ* soil moisture, for all SMOS–MODIS combinations in Table I, in Fig. 7. These results indicate that this prototype of the SMOS soil moisture processor was particularly underestimating soil moisture within the region under study. Hence, to proceed with the validation exercise, the SMOS soil moisture maps were re-scaled following the regression in Fig. 7, to remove the apparent dry bias. After re-scaling, the SMOS soil moisture data over Yanco has a coefficient of correlation R^2 with *in situ* data of 0.33 and root-mean-square-error (RMSE) of 0.16 $\mathrm{m}^3/\mathrm{m}^3$ (0 bias, 0.16 $\mathrm{m}^3/\mathrm{m}^3$ standard deviation).

Fig. 8 illustrates the performance of the downscaling algorithm using re-scaled SMOS soil moisture data over the Yanco region. Disaggregated soil moisture at 10 km is plotted against 10 km aggregated *in situ* soil moisture in Fig. 8(a). The histogram of the difference between 10 km downscaled and 10 km aggregated *in situ* soil moisture using the linking model in (2) and the linking model in (6) are presented in Fig. 8(b) and (c), respectively. Similarly, downscaling results at 1 km spatial resolution are presented in Fig. 8(d)–(f). From the regression plots, it can be seen that the sensitivity of the L2 product to soil moisture is reproduced at the scale of 10 km ($R^2 \sim 0.26$–0.30), but only partially reproduced at 1 km ($R^2 \sim 0.14$–0.21). The downscaled soil moisture maps when using (2) present a high bias, which is significantly reduced when using (6). The bias obtained when using the linking model in (2) is due to gradients in soil moisture captured by SMOS but not captured by MODIS, as shown in Fig. 3. The bias still present when using (6) is due to low resolution pixels that only have partial coverage of VIS/IR data at high resolution; it is controlled and does not appear when only pixels with full T_s coverage are employed. From these results, the RMSE when going into higher spatial resolutions is improved when adding SMOS T_B to the linking model, and is moderate when not adding them.

V. Conclusion

An algorithm for improving the spatial resolution of SMOS soil moisture estimates using MODIS-derived NDVI and T_s

data has been presented. Results of its application to SMOS imagery over Australia acquired during the commissioning phase indicate that with this technique it is feasible to improve the spatial resolution of SMOS accurate soil moisture retrievals. SMOS-derived soil moisture maps at 10 and 1 km have been obtained and results show that the soil moisture variability is nicely captured at the different spatial scales. Results from comparison with ground-based soil moisture measurements indicate that there is no a significant degradation of the RMSE when going into higher spatial resolutions; soil moisture sensitivity is preserved at 10 km and moderately decreased at 1 km. Further research using 1 km L-band passive airborne data collected during AACES is needed to fully validate the accuracy of the retrievals at every spatial resolution and establish the downscaling limit.

Now that SMOS has been successfully deployed in orbit, and its capabilities have been demonstrated during the commissioning phase, this work could potentially contribute to enhance the spatial resolution of SMOS soil moisture estimates, which will be a new and highly relevant research development. Also, these results suggest the prospect use of a VIS/IR sensor as a secondary payload in follow-on space-borne missions dedicated to soil moisture monitoring; the VIS/IR sensor could be highly useful in both the estimation of collocated land surface temperatures to be used in the soil moisture retrievals, and the improvement of the spatial resolution of the estimates using the universal triangle concept.

ACKNOWLEDGMENT

The authors would like to thank Arnaud Mialon for the assitance provided with the preliminary SMOS soil moisture products.

REFERENCES

[1] E. Njoku and D. Entekhabi, "Passive microwave remote sensing of soil moisture," *J. Hydrol.*, vol. 184, no. 1/2, pp. 101–129, Oct. 1996.

[2] T. Schmugge, W. Kustas, J. Ritchie, T. Jackson, and A. Rango, "Remote sensing in hydrology," *Adv. Water Resour.*, vol. 25, no. 8–12, pp. 1367–1385, Aug.–Dec. 2002.

[3] W. Wagner, G. Blsch, P. Pampaloni, J. Calvet, B. Bizarri, J. Wigneron, and Y. Kerr, "Operational readiness of microwave remote sensing of soil moisture for hydrologic applications," *Nordic Hydrol.*, vol. 38, no. 1, pp. 1–20, 2007.

[4] Y. Kerr, P. Waldteufel, J.-P. Wigneron, S. Delwart, F. Cabot, J. Boutin, M.-J. Escorihuela, J. Font, N. Reul, C. Gruhier, S. Juglea, M. R. Drinkwater, A. Hahne, M. Martin-Neira, and S. Mecklenburg, "The SMOS mission: New tool for monitoring key elements of the global water cycle," *Proc. IEEE*, vol. 98, no. 5, pp. 666–687, May 2010.

[5] D. Entekhabi, G. Asrar, A. Betts, K. Beven, R. Bras, C. Duffy, T. Dunne, R. S. Koster, D. Lettenmaier, D. McLaughlin, W. Shuttleworth, M. van Genuchten, M. Wei, and E. Wood, "An agenda for land surface hydrology research and a call for the second international hydrological decade," *Bull. Amer. Meteorol. Soc.*, vol. 80, no. 10, pp. 2043–2058, 1999.

[6] W. Crow, E. Wood, and R. Dubayah, "Potential for downscaling soil moisture maps derived from spaceborne imaging radar data," *J. Geophys. Res.*, vol. 105, no. D2, pp. 2203–2212, 2000.

[7] D. Entekhabi, E. Njoku, P. O'Neill, K. Kellogg, W. Crow, W. Edelstein, J. Entin, S. Goodman, T. Jackson, J. Johnson, J. Kimball, J. Piepmeier, R. Koster, K. McDonald, M. Moghaddam, S. Moran, R. Reichle, J. C. Shi, M. Spencer, S. Thurman, L. Tsang, and J. V. Zyl, "The Soil Moisture Active and Passive (SMAP) mission," *Proc. IEEE*, vol. 98, no. 5, pp. 704–716, May 2010.

[8] M. Piles, D. Entekhabi, and A. Camps, "A change detection algorithm for retrieving high-resolution soil moisture from SMAP radar and radiometer observations," *IEEE Trans. Geosci. Remote Sens.*, vol. 47, no. 12, pp. 4125–4131, Dec. 2009.

[9] N. N. Das, D. Entekhabi, and E. G. Njoku, "An algorithm for merging SMAP radiometer and radar data for high resolution soil moisture retrieval," *IEEE Trans. Geosci. Remote Sens.*, vol. 49, no. 5, pp. 1504–1512, May 2011.

[10] B. Idso, T. Schmugge, R. Jackson, and R. Reginto, "The utility of surface temperature measurements for remote sensing os foil water studies," *J. Geophys. Res.*, vol. 80, pp. 3044–3049, 1975.

[11] J. Price, "Thermal inertia mapping: A new view of the Earth," *J. Geophys. Res.*, vol. 82, no. 18, pp. 2582–2590, 1977.

[12] J. Adegoke and A. Carleton, "Relations between soil moisture and satellite vegetation indices in the U.S. corn belt," *J. Hydrometeor.*, vol. 3, no. 4, pp. 395–405, Aug. 2002.

[13] X. Wang, H. Xie, H. Guan, and X. Zhou, "Different responses of MODIS-derived NDVI to root-zone soil moisture in semi-arid and humid regions," *J. Hydrol. Earth Syst. Sci.*, vol. 340, no. 1/2, pp. 12–14, Jun. 2007.

[14] A. Cracknell and Y. Xue, "Thermal inertia determination from space—A tutorial review," *Int. J. Remote Sens.*, vol. 17, no. 3, pp. 431–461, Feb. 1996.

[15] Y. Zhang and M. Wegehenkel, "Integration of MODIS data into a simple model for the spatial distributed simulation of soil water content and evapotranspiration," *Remote Sens. Environ.*, vol. 104, no. 4, pp. 393–408, Oct. 2006.

[16] T. Carlson, "An overview of the 'triangle method' for estimating surface evapotranspiration and soil moisture from satellite imagery," *Sensors*, vol. 7, no. 8, pp. 1612–1629, 2007.

[17] G. Petropoulos, T. Carlson, M. Wooster, and S. Islam, "A review of Ts/VI remote sensing based methods for the retrieval of land surface energy fluxes and soil surface moisture," *Prog. Phys. Geography*, vol. 33, no. 2, pp. 224–250, Apr. 2009.

[18] X. Zhan, S. Miller, N. Chauhan, L. Di, and P. Ardanuy, "Soil moisture visible/infrared radiometer suite algorithm theoretical basis document," Raytheon Syst. Company, Lanham, MD, 2002, Tech. Rep.

[19] T. Carlson, R. Gillies, and E. Perry, "A method to make use of thermal infrared temperature and NDVI measurements to infer surface soil water content and fractional vegetation cover," *Remote Sens. Rev.*, vol. 9, no. 1/2, pp. 161–173, Mar. 1994.

[20] N. Chauhan, S. Miller, and P. Ardanuy, "Spaceborne soil moisture estimation at high resolution: A microwave-optical/IR synergistic approach," *Int. J. Remote Sens.*, vol. 24, no. 22, pp. 4599–4622, Nov. 2003.

[21] O. Merlin, J. Walker, A. Chehbouni, and Y. Kerr, "Towards deterministic downscaling of SMOS soil moisture using MODIS derived soil evaporative efficiency," *Remote Sens. Environ.*, vol. 112, no. 10, pp. 3935–3946, Oct. 2008.

[22] O. Merlin, A. Chehbouni, Y. Kerr, E. Njoku, and D. Entekhabi, "A combined modeling and multispectral/multiresolution remote sensing approach for disaggregation of surface soil moisture: Application to SMOS configuration," *IEEE Trans. Geosci. Remote Sens.*, vol. 43, no. 9, pp. 2036–2050, Sep. 2005.

[23] O. Merlin, A. Chehbouni, J. Walker, R. Panciera, and Y. Kerr, "A simple method to disaggregate passive microwave-based soil moisture," *IEEE Trans. Geosci. Remote Sens.*, vol. 46, no. 3, pp. 786–796, Mar. 2008.

[24] M. Piles, A. Camps, M. Vall-llossera, N. Sánchez, J. Martínez-Fernández, A. Monerris, G. Baroncini-Turricchia, C. Pérez-Gutiérrez, A. Aguasca, R. Acevo, and X. Bosch-Lluís, "Soil moisture downscaling activities at the REMEDHUS Cal/Val site and its application to SMOS," in *Proc. 11th Spec. Meeting Microw. Radiometry Remote Sens. Environ.*, 2010, pp. 17–21.

[25] S. Peischl, J. Walker, M. Allahmoradi, D. Barett, R. Gurney, Y. Kerr, E. Kim, J. LeMarshall, C. Rüdiger, D. Ryu, and N. Yeoh, "Towards validation of SMOS using airborne and ground data over the Murrumbidgee catchment," in *Proc. MODSIM Conf.*, 2009, pp. 3733–3739.

[26] R. Young, J. Walker, N. Yeoh, A. Smith, K. Ellett, O. Merlin, and A. Western, "Soil moisture and meteorological observations from the Murrumbigdee catchment," Dept. Civil Environ. Eng., Univ. Melbourne, Melbourne, Australia, 2008, Tech. Rep.

[27] K. McMullan, M. Brown, M. Martín-Neira, W. Rits, J. Martí, and J. Lemanczyk, "SMOS: The payload," *IEEE Trans. Geosci. Remote Sens.*, vol. 46, no. 3, pp. 594–605, Mar. 2008.

[28] F. Ulaby, R. Moore, and A. Fung, *Microwave Remote Sensing Active and Passive*, vol. 1/2. Norwood, MA: Artech House, 1981.

[29] G. Gutman and A. Ignatov, "The derivation of the green vegetation fraction from noaa/avhrr data for use in numerical weather prediction models," *Int. J. Remote Sens.*, vol. 19, no. 8, pp. 1533–1543, 1998.

[30] F. Baret, J. Clevers, and M. Stevens, "The robustness of canopy gap fraction estimations from red and near-infrared reflectances:

A comparison of approaches," *Remote Sens. Environ.*, vol. 54, no. 2, pp. 141–151, Nov. 1995.

[31] T. Carlson and D. Ripley, "On the relation between NDVI, fractional vegetation cover, and leaf area index," *Remote Sens. Environ.*, vol. 62, no. 3, pp. 241–252, Dec. 1997.

María Piles (S'05–M'11) was born in Valencia, Spain, in 1982. She received the M.S. and Ph.D. degrees in telecommunication engineering from the Universitat Politècnica de València, València, in 2005 and Universitat Politècnica de Catalunya (UPC), Barcelona, Spain, in 2010, respectively.

In 2004–2005, she was at Lund Institute of Technology, Lund, Sweden, with an Erasmus fellowship, where she pursued her undergraduate thesis on wireless networks and applications. In October 2005, she joined the Remote Sensing Laboratory, Department of Signal Theory and Communications, UPC, where she worked toward her Ph.D. with a FPU Grant from the Spanish Ministry of Science and Technology. Her research work has been mainly developed in the framework of the ESA SMOS and the NASA SMAP missions. She has been involved in the retrieval of soil moisture from SMOS radiometric measurements, in both numerical and experimental studies, and in the development of pixel disaggregation techniques to improve the spatial resolution of soil moisture estimates. In 2008, she was a visiting Ph.D. student at the Department of Civil and Environmental Engineering, Massachusetts Institute of Technology, Boston, where she worked on a downscaling algorithm to combine SMAP active and passive microwave measurements into high-resolution soil moisture estimates. In 2010, she joined the Department of Civil and Environmental Engineering, University of Melbourne, Australia, as a Research Fellow, working on SMOS soil moisture validation and downscaling. Her research interests include remote sensing for earth observation, interferometric radiometry, radar and VIS/IR sensors, soil moisture retrieval, pixel disaggregation techniques and data fusion.

Adriano Camps (S'91–A'97–M'00–SM'03–F'11) was born in Barcelona, Spain, in 1969. He received the M.S. and Ph.D. degrees in telecommunications engineering from the Universitat Politècnica de Catalunya (UPC), Barcelona, Spain, in 1992 and 1996, respectively.

In 1991 to 1992, he was at the ENS des Télécommunications de Bretagne, France, with an Erasmus Fellowship. Since 1993, he has been with the Electromagnetics and Photonics Engineering Group, Department of Signal Theory and Communications, UPC, where he was first Assistant Professor, Associate Professor in 1997, and Full Professor since 2007. In 1999, he was on sabbatical leave at the Microwave Remote Sensing Laboratory, of the University of Massachusetts, Amherst. Since 1993, he has been deeply involved in the European Space Agency SMOS Earth Explorer Mission, from the instrument and algorithmic points of view, performing field experiments, and more recently studying the use of GNSS-R techniques to perform the sea state correction needed to retrieve salinity from radiometric observations. His research interests are focused in microwave remote sensing, with special emphasis in microwave radiometry by aperture synthesis techniques and remote sensing using signals of opportunity (GNSS-R).

Dr. Camps was Chair of u Cal 2001, Technical Program Committee Cochair of IGARSS 2007, and co-chair of GNSS-R '10. Currently, he is Associate Editor of Radio Science and the IEEE TRANSACTIONS ON GEOSCIENCE AND REMOTE SENSING, and President-Founder of the IEEE Geoscience and Remote Sensing Society Chapter at Spain. In 1993, he received the Second National Award of University Studies; in 1997, the INDRA award of the Spanish Association of Telecommunication Engineers to the best Ph.D. in Remote Sensing; in 1999 the Extraordinary Ph.D. Award at the Universitat Politècnica de Catalunya; in 2002, the Research Distinction of the Generalitat de Catalunya for contributions to microwave passive remote sensing; and in 2004 he received a European Young Investigator Award, and in 2009 the ICREA Academia award. Moreover, as a member of the Microwave Radiometry Group, UPC, he received in 2000, 2001, and 2004: the 1st Duran Farell and the Ciutat de Barcelona awards for Technology Transfer, and the "Salvà i Campillo" Award of the Professional Association of Telecommunication Engineers of Catalonia for the most innovative research project for MIRAS/SMOS related activities, and in 2010 the 7th Duran Farell award for Technological Research for the work on GNSS-R instrumentation and applications. He has published nearly 100 papers in peer-reviewed journals, and more than 200 international conference presentations.

Mercè Vall-llossera (M'99) received the M.S. and Ph.D. degrees in telecommunications engineering from the Universitat Politècnica de Catalunya, UPC, Barcelona, Spain, in 1990 and 1994, respectively.

She has been lecturing and doing research at the Department of Signal Theory and Communications, UPC, from 1990 until 1997, as Assistant Professor and from 1997 until present, as Associate Professor. She spent a sabbatical year at the Concordia University, Montreal, QC, Canada, with the scholarship of the "Programme Québécois de Bourses d'excellence" (1996–1997): "Stages de Formation postdoctorale au Québec pour jeunes diplômés étrangers" applying the FDTD method in the analysis of the effect of mobile telephone to the body. At the beginning her research activities were related to numerical methods in electromagnetics and antenna analysis and design. At present, from 2000, her research is ainly related to passive remote sensing, geophysical parameters retrieval: soil moisture and ocean salinity retrieval from L-band radiometric measurements. She has been participating in several projects for the preparation of the Soil Moisture and Ocean Salinity (SMOS) mission by ESA.

Ignasi Corbella (S'78–M'82–SM'08) was born in Barcelona, Spain, in 1955. He received the M.S. and Ph.D. degrees in telecommunications engineering from the Universitat Politècnica de Catalunya (UPC), Barcelona, Spain, in 1977 and 1983, respectively.

In 1976, he was with the School of Telecommunication Engineering, UPC, as a Research Assistant in the Microwave Laboratory, where he worked on passive microwave integrated-circuit design and characterization. In 1979, he was with Thomson-CSF, Paris, France, on microwave oscillators design. In 1982, he was an Assistant Professor, in 1986, an Associate Professor, and in 1993, a Full Professor with UPC, where he is currently teaching basic microwaves and antennas at undergraduate level and graduate courses on nonlinear microwave circuits. Since 1993, he has been actively participating as a Researcher with the European Space Agency (ESA) SMOS mission in the frame of several contracts, directly with ESA, or with the payload prime contractor EADS-Casa Espacio. His expertise includes, among others, fundamentals of interferometric aperture synthesis radiometry, image reconstruction algorithms, and onboard calibration, hardware specification, and payload characterization. From 1993 to 1997, he was an Academic Director with the School of Telecommunications Engineering. From 2001 to 2003, he was a Director with the Department of Signal Theory and Communications, UPC. From 1998 to 1999, he was with the NOAA/Environmental Technology Laboratory, as a Guest Researcher developing methods for total-power radiometer calibration and data analysis. From 1999 to 2007, he was the Scientific Coordinator of a Dictionary of Telecommunication terms in Catalan language, with more than 4 000 entries, published in March 2007. Since 2004, he has been a member of the SMOS Science Advisory Group, and since 2007, he has been a member of the SMOS Barcelona Expert Centre.

Dr. Corbella was the General Chairman of the 2007 International Geoscience and Remote Sensing Symposium (IGARSS'07), Barcelona.

Rocco Panciera received the M.S. degree in environmental engineering from the University of Trento, Trento, Italy, in 2003 and the Ph.D. degree from the University of Melbourne, Melbourne, Australia, in 2009.

He was a Research Fellow at the University of Melbourne, from 2009 to 2011, working on active and passive microwave soil moisture retrieval for the Soil Moisture Active Passive (SMAP) mission. He is currently employed by the Cooperative Research Centre for Spatial information, Australia, under a Superscience Fellowship from the Australian Research Council (ARC). His current research focuses on the retrieval of near-surface soil moisture from active microwave observations.

Christoph Rüdiger (M'10) received the B.E. degree in civil engineering from the University of Applied Sciences of Wiesbaden, Wiesbaden, Germany, in 2002 and the Ph.D. degree in environmental engineering from the University of Melbourne, Melbourne, Australia, in 2007, studying the potential to assimilate streamflow data into land surface models for soil moisture prediction.

His undergraduate thesis covered the topic of groundwater and contaminant flow around future buildings. He then joined the Centre National de Recherches Météorologiques (CNRM) at Météo France in Toulouse to work on the preparation of surface soil moisture and LAI data assimilation into the French land surface model ISBA. During this period he also worked on the validation of different passive and active microwave satellite products over France, with a particular focus on SMOS. Since his return to Australia in July 2008, he has coordinated and led a number of cal/val campaigns for the Australian land validation segment of ESA's SMOS mission in the Australian arid zone and the Murrumbidgee River catchment. In addition to this, he continues to work on land surface data assimilation and also participates in the Australian cal/val campaigns for SMAP and Aquarius. He now works at Monash University in Melbourne.

Yann H. Kerr (M'88–SM'01), received the B.S. degree in engineering from Ecole Nationale Supérieure de l'Aéronautique et de l'Espace (ENSAE), Malakoff, France, the M.Sc. degree from Glasgow University in E& EE, Scotland, U.K., and the Ph.D. degree from Université Paul Sabatier, Toulouse, France.

From 1980 to 1985, he was employed by CNES. In 1985, he joined LERTS; for which he was Director, in 1993–1994. He spent 19 months at JPL, Pasadena in 1987–1988. He has been working at CESBIO, since 1995 (deputy director and director since 2007). His fields of interest are in the theory and techniques for microwave and thermal infra-red remote sensing of the earth, with emphasis on hydrology, water resources management and vegetation monitoring. He has been involved with many space missions. He was an EOS principal investigator (interdisciplinary investigations) and precursor of the use of the SCAT over land. In 1989, he started to work on the interferometric concept applied to passive microwave earth observation and was subsequently the science lead on the MIRAS project for ESA with MMS and OMP. He was also a Co Investigator on IRIS, OSIRIS and HYDROS for NASA. He was Science Advisor for MIMR and Co I on AMSR. He is a member of the SMAP science definition team. In 1997, he first proposed the natural outcome of the previous MIRAS work with what was to become the SMOS Mission which was selected by ESA, in 1999, with him as the SMOS mission Lead-Investigator and Chair of the Science Advisory Group. He is also in charge of the SMOS science activities coordination in France. He has organized all the SMOS workshops, and was Guest Editor on two IEEE Special issues.

Jeffrey Walker received the B.E. (Civil) and B.Surveying degrees with Hons 1 and University Medal from the University of Newcastle, Australia, in 1995, and the Ph.D. in water resources engineering from the University of Newcastle, in 1999.

His Ph.D. thesis was among the early pioneering research on estimation of root-zone soil moisture from remotely sensed surface soil moisture observations. He then joined NASA Goddard Space Flight Centre to implement his soil moisture work globally. In 2001, he moved to the Department of Civil and Environmental Engineering at the University of Melbourne as Lecturer, where he continued his soil moisture work, including development of the only Australian airborne capability for simulating new satellite missions for soil moisture. In 2010, he was appointed as Professor in the Department of Civil Engineering at Monash University where he is continuing this research. He is contributing to soil moisture satellite missions at both NASA and ESA, as a Science Definition Team member for the Soil Moisture Active Passive (SMAP) mission and Cal/val Team member for the Soil Moisture and Ocean Salinity (SMOS) mission, respectively.